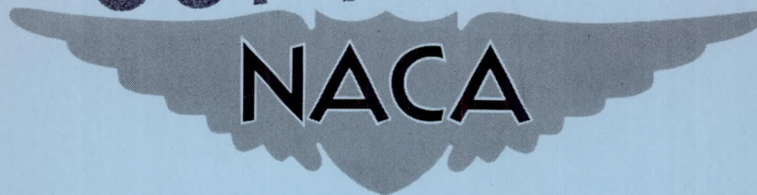


NACA RM E55G19

RM E55G19

**CASE FILE  
COPY**



# RESEARCH MEMORANDUM

INTERACTION OF A JET AND FLAT PLATE

LOCATED IN AN AIRSTREAM

By Gerald W. Englert, Joseph F. Wasserbauer,  
and Paul Whalen

Lewis Flight Propulsion Laboratory  
Cleveland, Ohio

**NATIONAL ADVISORY COMMITTEE  
FOR AERONAUTICS  
WASHINGTON**

September 8, 1955  
Declassified December 1, 1959

## NATIONAL ADVISORY COMMITTEE FOR AERONAUTICS

RESEARCH MEMORANDUM

## INTERACTION OF A JET AND FLAT PLATE LOCATED IN AN AIRSTREAM

By Gerald W. Englert, Joseph F. Wasserbauer, and Paul Whalen

## SUMMARY

The interaction between a flat plate and a nearby jet issuing from a convergent nozzle was studied over a range of pressure ratios from jet-off to 9 and at free-stream Mach numbers of 0.1, 0.6, 1.6, and 2.0. The effect on this interaction of the presence of streamline, blunt-base, and curved-base fairings between the plate and parabolic afterbody housing the exit nozzle was also investigated. The plate was located at various distances from and at various angles with respect to the nozzle axis of symmetry.

The jet deflection was about  $3^\circ$  when measured at a pressure ratio of 5 and a free-stream Mach number of 2.0. Addition of fairings, especially those with curved or blunt bases, increased this angle considerably, decreased the average pressure on the plate, and shifted the center of pressure rearward. Largest pressure gradients on the plate were due to the intersection of the plate with a boattail shock and with shocks originating within the jet stream. Change of exit-nozzle angles of attack from  $0$  to  $8^\circ$  toward the plate showed no large effect on the plate normal forces at a free-stream Mach number of 1.6 and a pressure ratio of 2.

## INTRODUCTION

In the design of jet-propelled airplanes or missiles it may at times be advantageous to locate the exhaust jet at positions other than the rearmost extremities of the airplane. However, drag, vibration, control, and cooling problems may then become especially complicated because of the interaction of the jet and nearby airframe surfaces (refs. 1 and 2). Several studies have been made of the influence of an exhaust jet on wings (refs. 3 and 4) and tail fins (refs. 5, 6, and 7).

The many different shapes, contours, and flow conditions about these airframe surfaces make generalization of results very difficult. This difficulty is increased because of the many different possible orientations of the jet with the nearby surfaces and the variety of exhaust nozzles or exhaust systems. Therefore, a preliminary study of a series

3794

1-10

of elementary contour surfaces and a jet from a simple converging nozzle was made to approach the problem. In attempting to eventually lead systematically to more complex cases, families of concave, convex, wedge-shaped, and flat plates were studied with various fairings installed in the region between the surfaces and the afterbody housing the exhaust nozzle.

This report presents the results of jet interference on a flat plate oriented at various distances from and at various angles to the nozzle axis of symmetry. The study was made over a range of pressure ratios and free-stream Mach numbers in the NACA Lewis 8- by 6-foot supersonic wind tunnel.

#### SYMBOLS

The following symbols are used in this report:

- A plan area of plate from nozzle-exit station to plate trailing edge station, 1.5 sq ft
- $C_p$  pressure coefficient,  $\frac{p - p_\infty}{q_\infty}$
- L length of plate from nozzle-exit station to plate trailing edge station, 1.5 ft
- $l$  distance to center of pressure from nozzle-exit station along surface of plate in chordwise direction
- M Mach number
- N force normal to plate, positive when directed toward the nozzle centerline
- P total pressure at nozzle entrance
- p static pressure
- q dynamic pressure
- r radius
- S axial distance from nozzle-entrance station
- V velocity
- w width of jet normal shock of first period

- x distance downstream of nozzle-exit station and parallel to free-stream direction
- Y vertical distance between plate leading edge and nozzle centerline
- y coordinate orthogonal to x and z coordinates
- z spanwise distance from midchord of plate
- $\alpha_m$  angle of attack of exit model with respect to free-stream direction, positive when nozzle is directed toward plate
- $\alpha_p$  angle of attack of plate with respect to free-stream direction, positive when nozzle centerline for  $\alpha_m = 0$  is farther from trailing edge than leading edge
- $\delta$  angle of jet deflection with respect to nozzle centerline, considered positive when jet deflects toward plate

## Subscripts:

- a afterbody
- j condition in jet when expanded isentropically and one-dimensionally over  $P/p_\infty$
- n nozzle
- ne nozzle exit
- w normal shock of first jet period
- $\infty$  free stream

## APPARATUS AND PROCEDURE

The jet was supplied by the exit-model apparatus reported in reference 8. The general layout of this model, the flat plate, and the support system are shown in figure 1. The dimensions of the convergent exit nozzle and parabolic afterbody are given in figure 2.

Part of the runs at zero model and plate angle of attack were made with biconvex circular-arc fairings between the exit model and flat plate (fig. 3). The aft ends of these fairings were terminated as either a sharp trailing edge, or a blunt, or curved base. The curved- and blunt-base fairings separated the plate a distance of 2.03 exit-nozzle radii from the nozzle centerline. Two sharp trailing-edge fairings set this distance at either 1.40 or 2.03 exit-nozzle radii. The plate was tangent to the exit model at its maximum body radius when this distance ratio was 2.03. The fineness ratio of these fairings was 3.

Static-pressure-measuring orifices were located on the plate as shown in figure 2. Two total- and static-pressure rakes were located at the trailing edge of the plate. Schlieren photographs were taken of the jet structure and flow over the plate.

Without fairings the plate was positioned at vertical distances of 1.0 to 5.6 nozzle-exit radii from the jet centerline, and at angles of attack of  $-8^\circ$ ,  $0^\circ$ ,  $8^\circ$ , and  $16^\circ$  with respect to the free-stream direction. The exit-model angle of attack was set at either  $0^\circ$  or  $+8^\circ$ .

Pressure inside the nozzle was varied from a jet-off value to values producing a pressure ratio  $P/p_\infty$  of 9 and the free-stream Mach number was set at 0.1, 0.6, 1.6, and 2.0.

## RESULTS AND DISCUSSION

### Influence of Plate and Fairings on Jet

Sketches of typical jet structure of a convergent nozzle operating at high pressure ratios in subsonic and supersonic free streams are shown in figure 4. With subsonic external flow, the jet structure is of a periodic nature and all shocks are restricted to within the jet stream. With supersonic external flow, the oblique shocks, which are formed near the nozzle exit, intersect with each other or with a normal shock, reflect, and then pass through the turbulent mixing zone and out into the external stream (ref. 9). No reflection of these shocks from the mixing zone back into the jet stream was observed.

Deflection of the jet toward the plate was the only effect of the plate surface or fairings with the plate outside the jet boundary. The width of the normal shock and its distance from the nozzle exit remained unchanged with the addition of the plate or fairings (fig. 5). These distances were in close agreement with the results of reference 9 for the case of the jet alone in quiescent air.

Schlieren photographs were used to determine the amount of deflection of the jet toward the plate. The angle between the nozzle axis and a line extending from the center of the nozzle exit to the intersection of the first two jet shocks (or to the midpoint of the normal shock if the two oblique shocks did not intersect with one another) is presented in figure 6. This angle was considered positive when the jet deflected toward the plate.

Deflection in the case of the plate without fairings was about  $3^\circ$  for a pressure ratio of 5 and a free-stream Mach number  $M_\infty$  of 2.0 (fig. 6(a)). The tendency of the jet to aspirate the region between the plate and jet and attach to the plate was counterbalanced by the intruding air

from the plate sides and leading edge. The presence of the blunt or curved bases permitted a low- or base-pressure zone near the jet exit at supersonic speeds. The jet in these cases deflected an appreciably greater amount. The effect of the streamlined fairings, although small, increased the deflection of the jet toward the plate beyond that of the plate alone.

In general, increasing the pressure ratio  $P/p_\infty$  increased jet deflection in the subsonic free-stream case and decreased deflection in the supersonic case. Typical results are shown in figure 6(b). Absence of shock patterns on the schlieren photographs prevented determination of the curve at low pressure ratios. Increased free-stream static pressure and a curtailed nozzle-supply pressure limited the subsonic curve at high pressure ratios.

#### Influence of Jet Fairings on Plate

The steepest pressure gradients measured on the plate in a supersonic free stream were due to shocks formed either within the jet or near the boattail trailing edge. Even with subsonic stream flow, appreciable pressure gradients were transmitted to the plate because of the deflection of the streamlines of the external flow passing over the jet.

Typical contour plots of the plate pressure distribution with the plate located 2.03 nozzle-exit radii from the nozzle centerline are shown in figure 7. The measured inlet total- to free-stream static-pressure ratio across the nozzle was 5. The increased pressures due to the jet shocks were usually restricted to narrower zones in the supersonic free-stream cases than in the subsonic case. Intersection of the shocks with the surface was calculated from schlieren photographs by the measured shock angle and axial position.

The normal force coefficient and the center of pressure location were determined by integrating the pressure distributions on the plate. Normal force was considered positive when acting from the plate toward the nozzle centerline.

The effect of vertical distance between the plate surface and nozzle centerline  $Y/r_{ne}$  at a free-stream Mach number of 1.6 is shown in figure 8. The pressure ratio across the nozzle was set at 2 so that no effect of jet shocks would be present. The distance to the center of moments increased because of a strong boattail shock striking the plate at increasing axial distances from the nozzle as the plate was lowered away from the jet. The plate pressure distributions showing the effect of the boattail shock are presented in figure 9.

Normal force approached zero, as expected, as  $Y/r_{ne}$  was increased beyond 2.03. As  $Y/r_{ne}$  was decreased below 1.4, however, the absolute

value of the normal forces decreased as the plate became submerged more and more into the jet stream. The static-pressure coefficient of the jet stream measured by the pressure rakes at the plate trailing edge, is marked by the  $x$  on figures 9(b) and (c).

The effect of nozzle pressure ratio on the plate is shown in figure 10. A  $Y/r_{ne}$  of 2.03 was selected as the boattail shock was far enough forward of the plate to cause very little contribution to the trends. When the jet was turned off, the pressure at the nozzle exit corresponded to that behind a blunt trailing-edge body. With a supersonic free stream, base pressure was well below free-stream values. This zone of low pressure was felt on the fore part of the plate and tended to decrease the absolute value of the normal force and shift the center of pressure rearward. As the jet was turned on, the pressure in these regions was increased. However, a low-pressure zone preceded the jet shock as the jet was overexpanded. Also, as the pressure ratio across the nozzle was increased, the shock pattern elongated in an axial direction (fig. 5) exposing more of the plate to the low-pressure region. This is believed to have caused the decreasing absolute value of the normal forces as the pressure ratio was increased at the high values.

The influence of fairings on the plate is shown in figure 11. The pressure integrations to obtain forces and moments for these configurations were made over the same projected area as that of the configurations which had no fairing. The low-pressure zone created by the blunt and curved fairings appreciably decreased the average pressure on the plate and shifted the center of moments rearward. Each test point of figure 11 was first set by increasing the nozzle pressure ratio from a low value to the value recorded. Some difference of forces and moments were then obtained for the plate with fairings by arriving at the test point by lowering the nozzle pressure ratio from a higher value. This hysteresis effect was especially apparent for the blunt- and curved-base configurations.

Only slight changes of the forces were noted by increasing the angle of attack of the exit model from  $0^\circ$  to  $8^\circ$  at a free-stream Mach number of 1.6 and a pressure ratio of 2 (fig. 12). This indicates that the jet may have turned in a free-stream direction very near the nozzle exit. Normal forces varied linearly with plate angle of attack from  $0^\circ$  to  $16^\circ$ , and the center of pressure changed somewhat erratically. It is possible, however, for small changes in pressure distribution to cause large changes in center of pressure location.

The effects of distance between the plate and nozzle centerline, of pressure ratio across the nozzle, and of fairings on the pressure fluctuations  $\left( \frac{p_{max} - p_{min}}{q_\infty} \right)$  at two points on the plate (see fig. 2) are shown

in figures 13, 14, and 15. The pressure-recording system used to obtain the data presented in these figures was accurate up to 100 cycles per second. Various frequency-amplitude surveys were made with equipment accurate to 1000 cycles per second. These measurements showed no resonant or especially large pressure amplitudes at any frequency, but showed instead a typical noise trace over the range studied. Pressure amplitude fluctuations of the order of 0.1 were observed on the plate.

The pressure amplitude was greater at the aft dynamic pickup location than at the fore location for the plate without fairings. This difference may have been due to the spreading of the jet to regions near the plate at the aft pickup location. The addition of fairings, however, increased the disturbances at the fore position and decreased those at the aft.

Pressure amplitudes of the fore pickup measured at a free-stream Mach number of 0.1 were of the same order of magnitude as the jet-noise data for a 1-inch-diameter jet alone in still air (ref 10). This comparison was made by use of the evaluation of reference 11 to correct the 1-inch-diameter jet data to the larger size exit of this investigation.

#### SUMMARY OF RESULTS

The following results were obtained by investigating the interaction of a flat plate, a jet issuing from an axisymmetric body, and fairings between the plate and body over a range of free-stream Mach numbers and pressure ratios across the exit nozzle:

1. With the plate at zero angle of attack, jet deflection of approximately  $3^\circ$  was obtained at a free-stream Mach number of 2.0 and a pressure ratio of 5. Installations of fairings between the plate and the exit models housing the exhaust nozzle increased the jet deflections which were always toward the plate.
2. Largest pressure gradients on the plate were due to the intersection of the plate surface with a boattail shock and with shocks originating within the jet stream.
3. The presence of fairings decreased the average pressure on the plate and shifted the center of pressure rearward.
4. Change of exit-nozzle angle of inclination from  $0^\circ$  to  $8^\circ$  toward the plate showed no large effects on plate normal forces at a free-stream Mach number of 1.6 and a pressure ratio of 2.
5. Pressure fluctuations on the plate as great as 0.1 were observed.



## REFERENCES

1. Squire, H. B.: Jet Flow and Its Effects on Aircraft. *Aircraft Eng.*, vol. XXII, no. 253, Mar. 1950, pp. 62-67.
2. Jonas, Julius: On the Interaction Between Multiple Jets and an Adjacent Surface. *Aero. Eng. Rev.*, vol. 11, no. 1, Jan. 1952, pp. 21-25.
3. Falk, H.: The Influence of the Jet of a Propulsion Unit on Nearby Wings. NACA TM 1104, 1946.
4. Bressette, Walter E.: Investigation of the Jet Effects on a Flat Surface Downstream of the Exit of a Simulated Turbojet Nacelle at a Free-Stream Mach Number of 2.02. NACA RM L54E05a, 1954.
5. Hatch, John E., Jr., and Savelle, William M.: Some Effects of a Sonic Jet Exhaust on the Loading over a Yawed Fin at a Mach Number of 3.03. NACA RM L52L02a, 1953.
6. Potter, J. Leith, and Shapiro, Norman M.: Some Effects of a Propulsion Jet on the Flow over the Fins of a Missile. Rep. 2R3F, Ord. Missile Labs., Redstone Arsenal, Jan. 11, 1954. (Proj. TB3-0108.)
7. Valerino, Alfred S.: Jet Effects on Pressure Loading of All-Movable Horizontal Stabilizer. NACA RM E54C24, 1954.
8. Englert, Gerald W., Vargo, Donald J., and Cubbison, Robert W.: Effect of Jet-Nozzle-Expansion Ratio on Drag of Parabolic Afterbodies. NACA RM E54B12, 1954.
9. Love, Eugene S., and Grigsby, Carl E.: Some Studies of Axisymmetric Free Jets Exhausting from Sonic and Supersonic Nozzles into Still Air and into Supersonic Streams. NACA RM L54L31, 1955.
10. Lassiter, Leslie W., and Hubbard, Harvey H.: The Near Noise Field of Static Jets and Some Model Studies of Devices for Noise Reduction. NACA TN 3187, 1954.
11. Sanders, Newell D., and North, Warren J.: Preliminary Evaluation of Two Methods for Reduction of Jet-Engine Noise. Paper presented at Inst. Aero. Sci. Meeting, Cleveland (Ohio), Mar. 12, 1954.

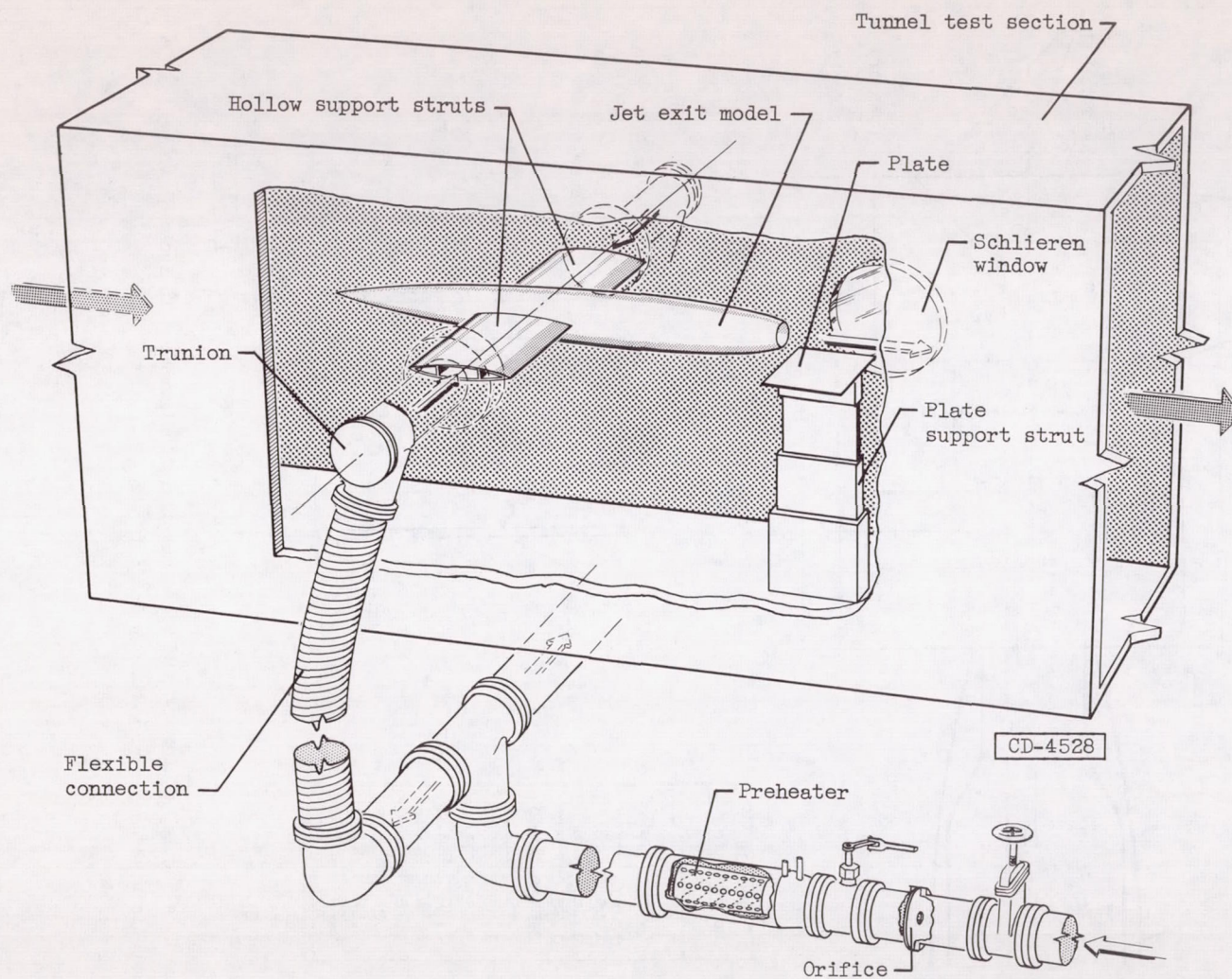
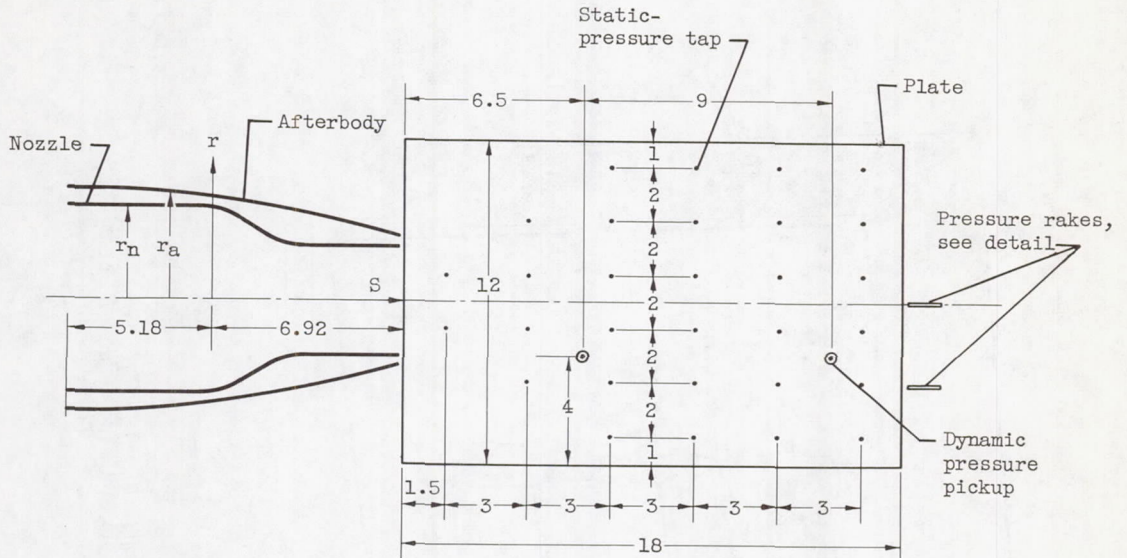


Figure 1. - Schematic drawing of interaction study model in 8- by 6-foot test section.



Nozzle coordinates	
S	r <sub>n</sub>
0	3.500
0.35	3.495
0.71	3.410
1.04	3.215
1.38	2.985
1.73	2.715
2.07	2.550
2.42	2.390
2.76	2.280
3.11	2.190
3.56	2.135
3.81	2.089
4.15	2.060
4.84	2.035
5.52	2.032
6.23	2.030
6.92	2.030

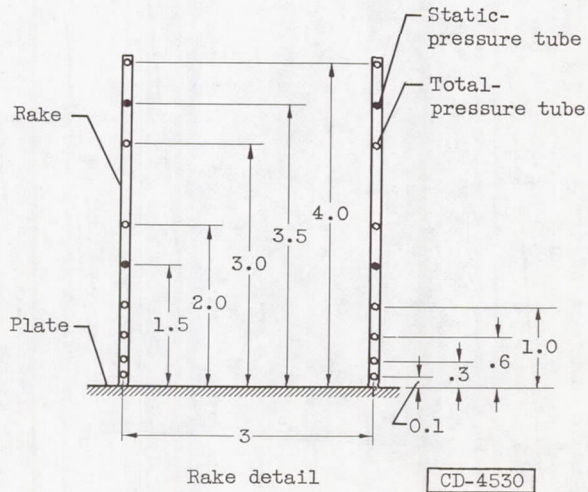


Figure 2. - Nozzle, afterbody, and plate detail (all dimensions in inches). Equation of parabolic afterbody:  $r_a = 4.125 - \frac{4.125}{18^2} (s + 5.18)^2$ .

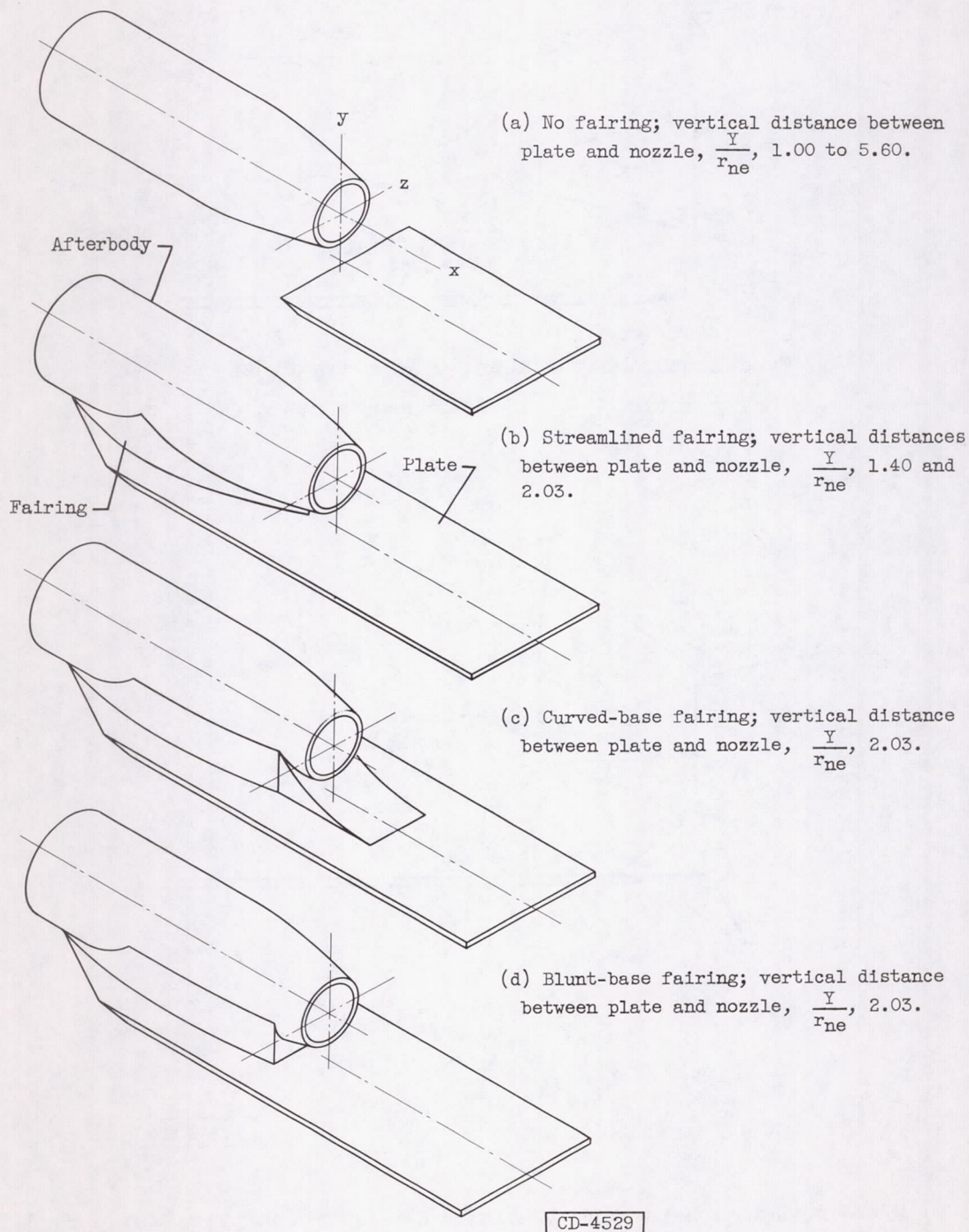
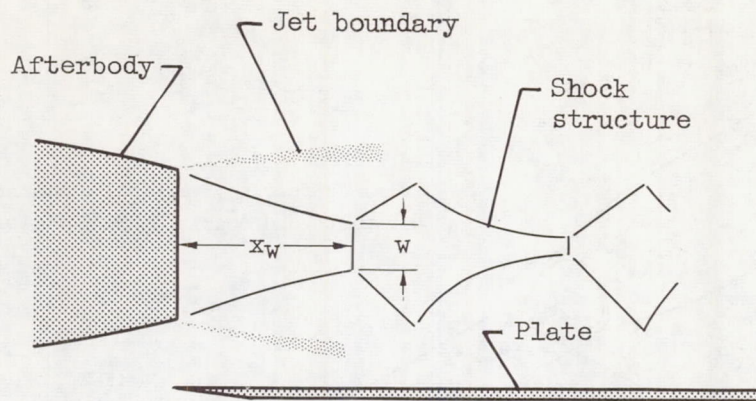
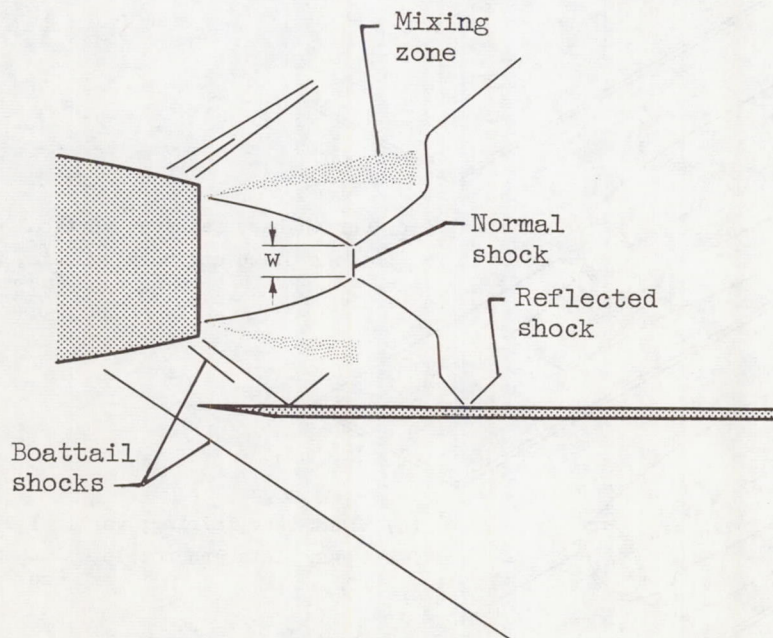


Figure 3. - Types of fairing between afterbody and plate.



(a) Free-stream Mach number, 0.1; average jet velocity ratio,  $\frac{V_j}{V_\infty}$ , 16.7; pressure ratio,  $\frac{P}{P_\infty}$ , 5.



CD-4536

(b) Free-stream Mach number, 1.6; average jet velocity ratio,  $\frac{V_j}{V_\infty}$ , 1.2; pressure ratio,  $\frac{P}{P_\infty}$ , 5.

Figure 4. - Typical jet structure.

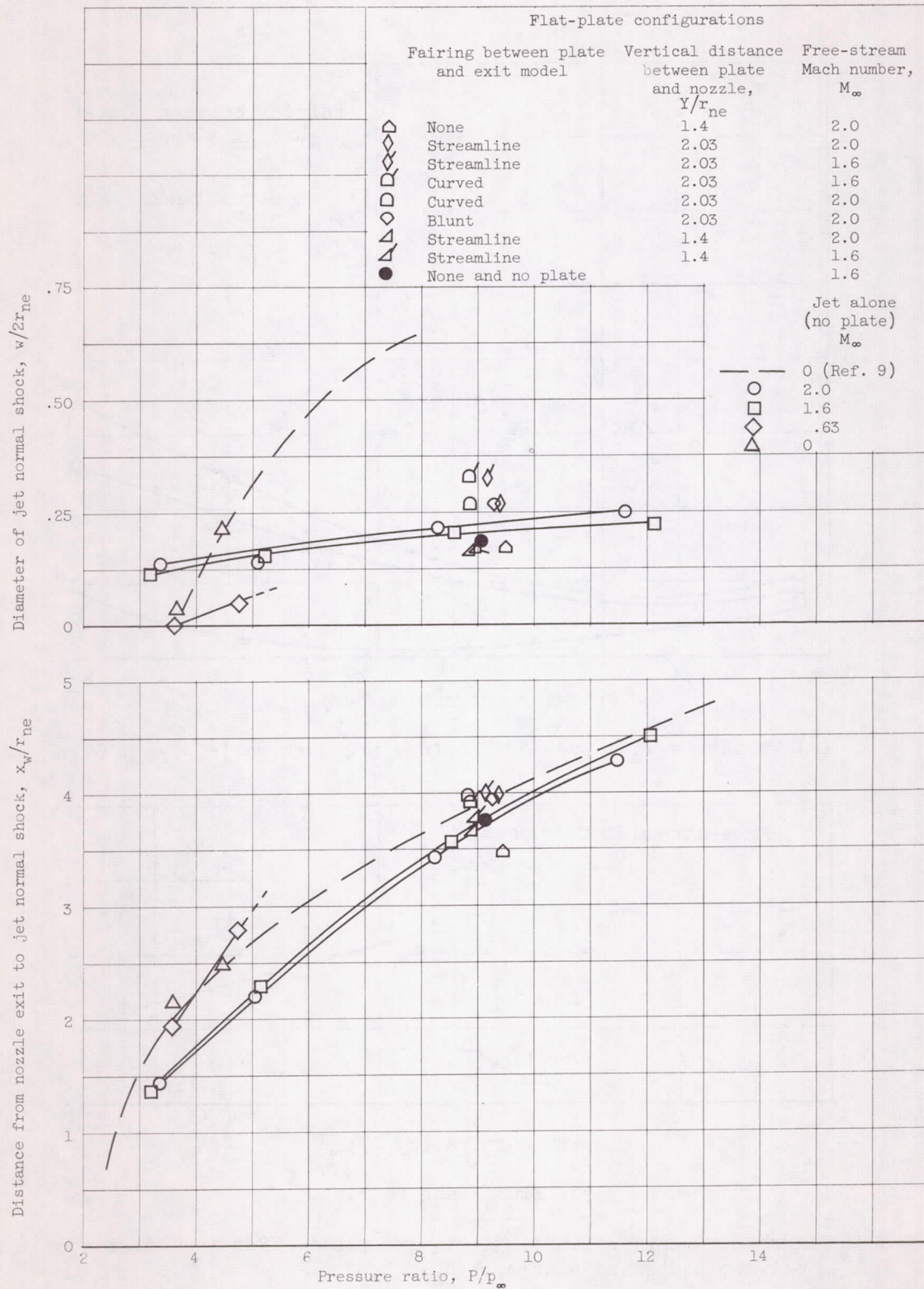
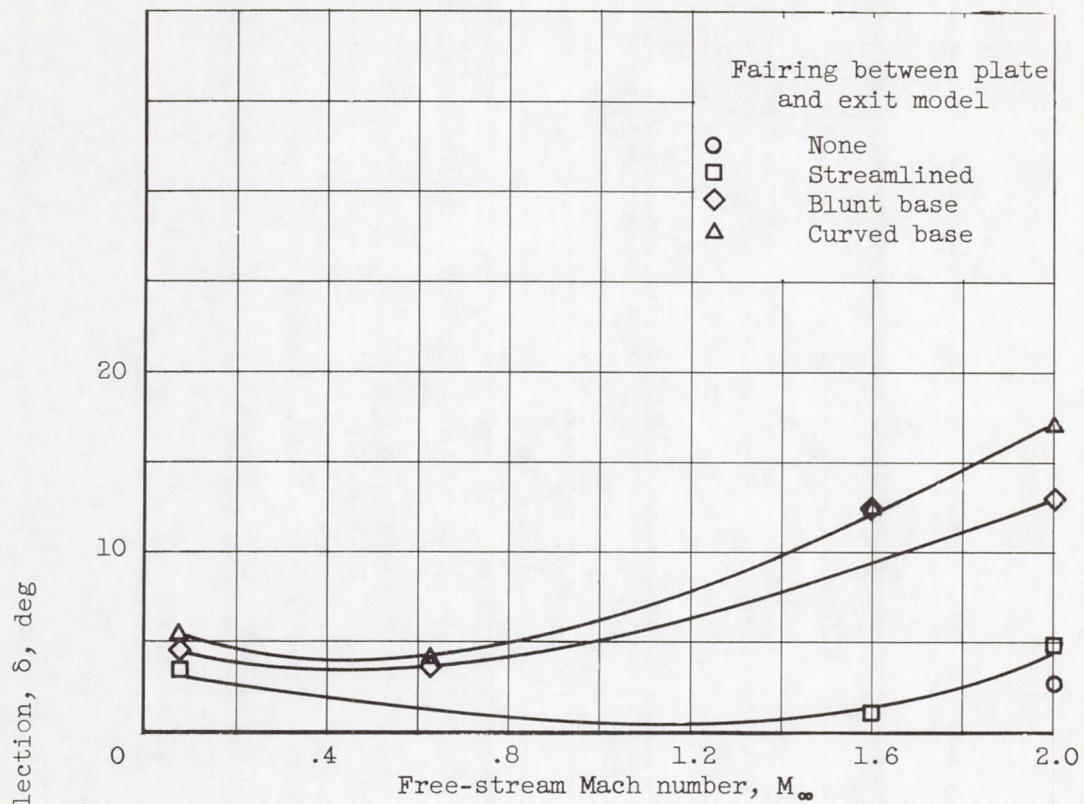
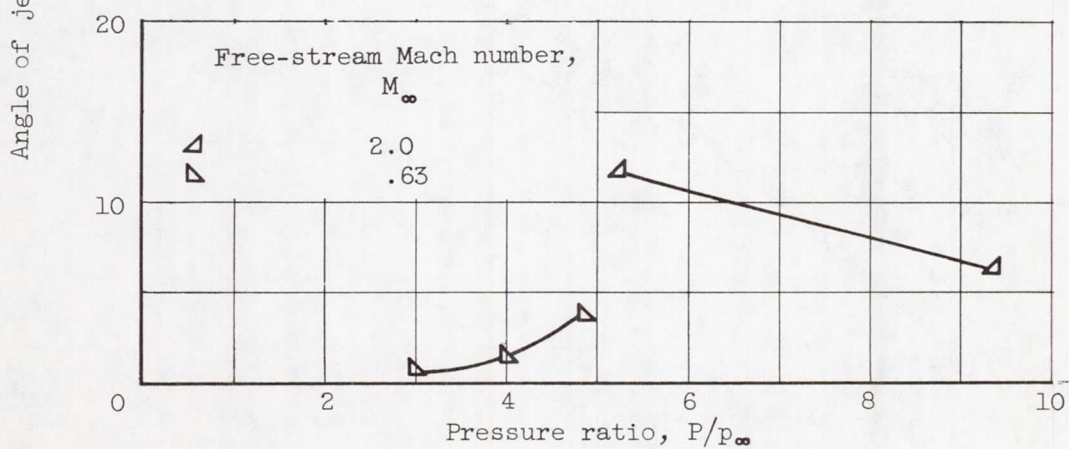
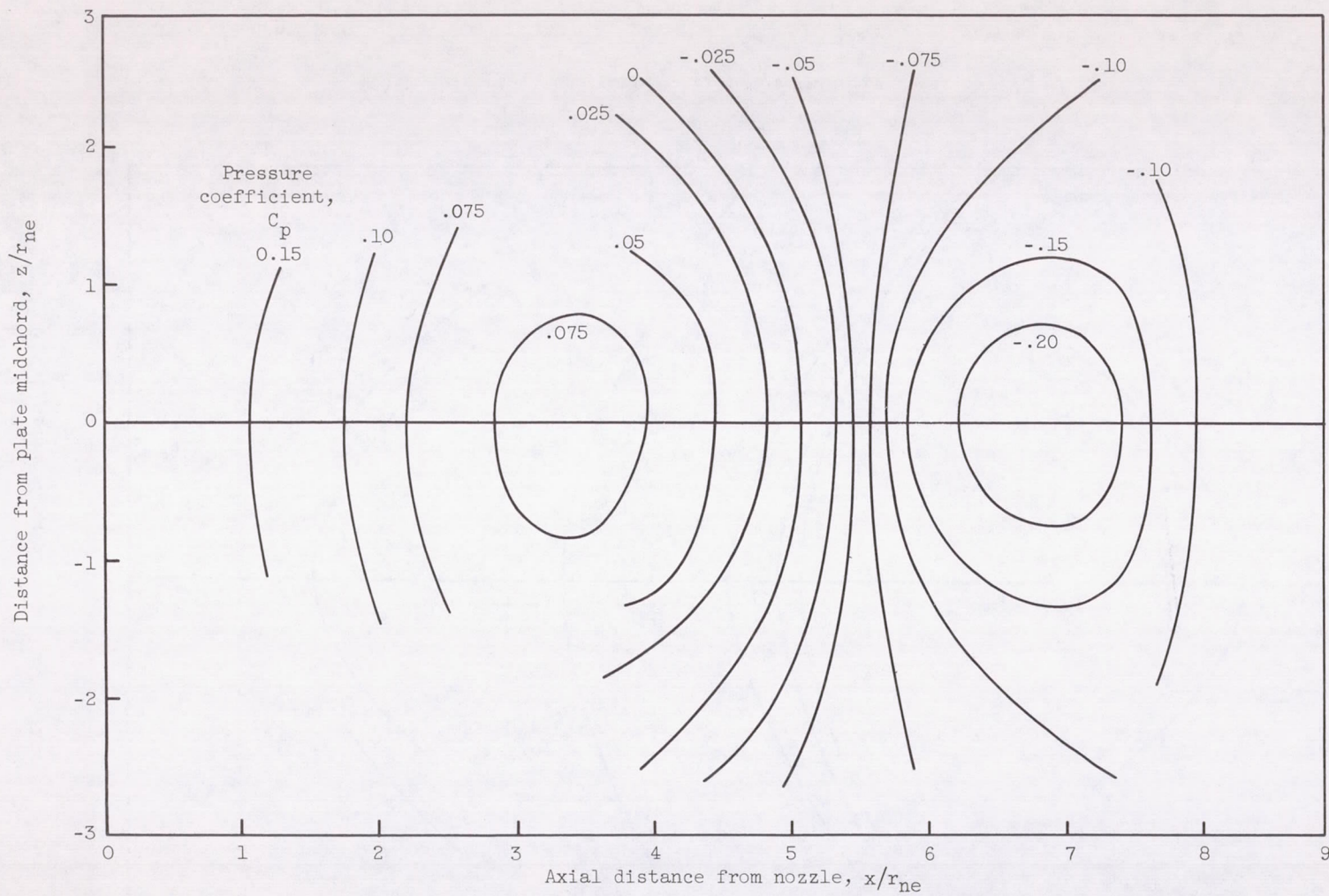


Figure 5. - Effect of plate and fairing on jet shock structure of first period.

(a) Variation with type of fairing; pressure ratio,  $P/p_\infty$ , 5.

(b) Blunt-base fairing.

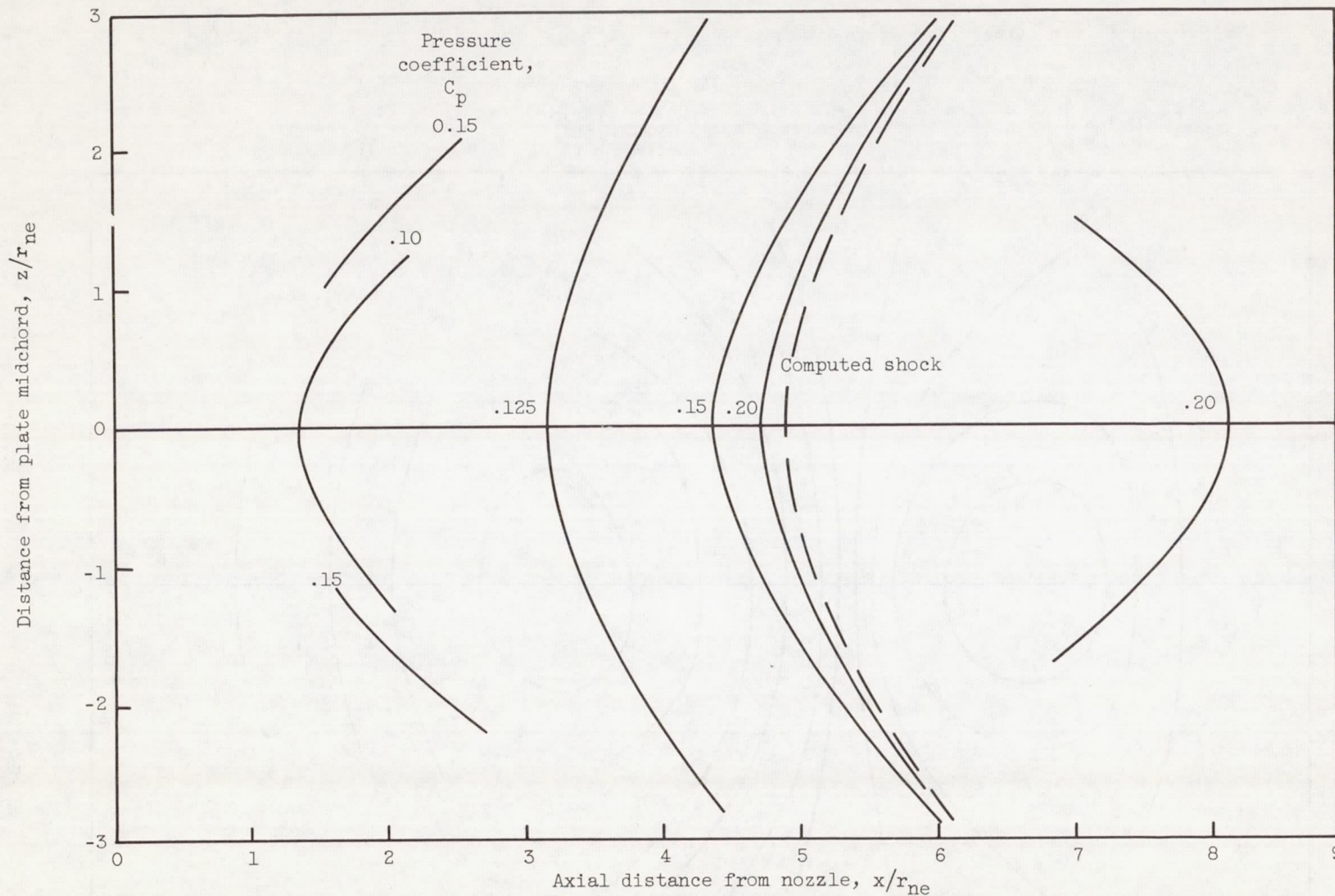
Figure 6. - Deflection of jet toward plate. Vertical distance between plate and nozzle,  $Y/r_{ne}$ , 2.03.



(a) Free-stream Mach number, 0.63; jet velocity ratio,  $V_j/V_\infty$ , 2.77.

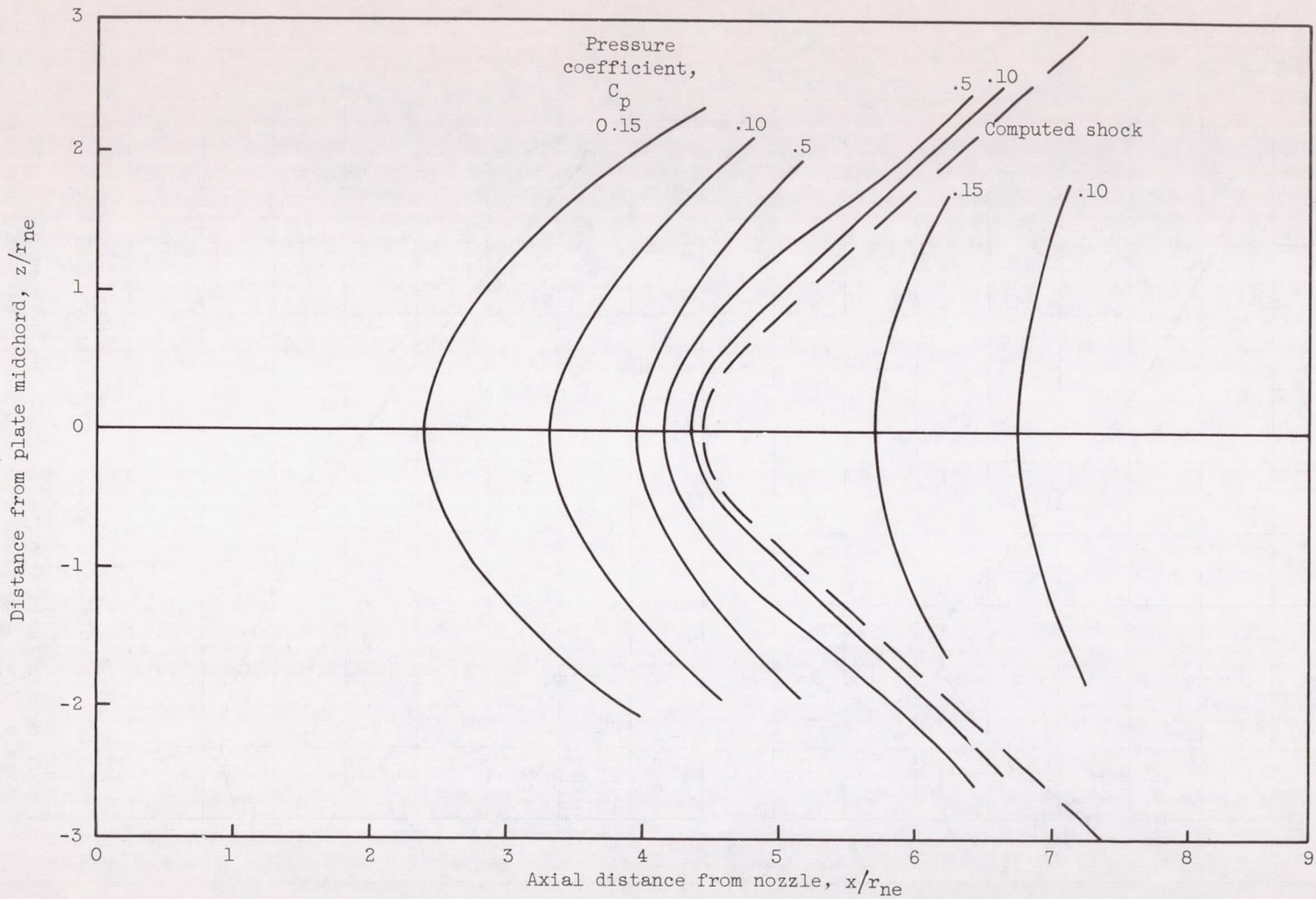
Figure 7. - Pressure contours on plate. Vertical distance between plate and nozzle,  $Y/r_{ne}$ , 2.03; pressure ratio,  $P/p_\infty$ , 5; streamlined fairing between plate and boattail of exit model.





(b) Free-stream Mach number, 1.6; jet velocity ratio,  $V_j/V_\infty$ , 1.28.

Figure 7. - Continued. Pressure contours on plate. Vertical distance between plate and nozzle,  $Y/r_{ne}$ , 2.03; pressure ratio,  $P/P_\infty$ , 5; streamlined fairing between plate and boattail of exit model.



(c) Free-stream Mach number, 2.0; jet velocity ratio,  $V_j/V_\infty$ , 1.07.

Figure 7. - Concluded. Pressure contours on plate. Vertical distance between plate and nozzle,  $Y/r_{ne}$ , 2.03; pressure ratio,  $P/P_\infty$ , 5; streamlined fairing between plate and boattail of exit model.

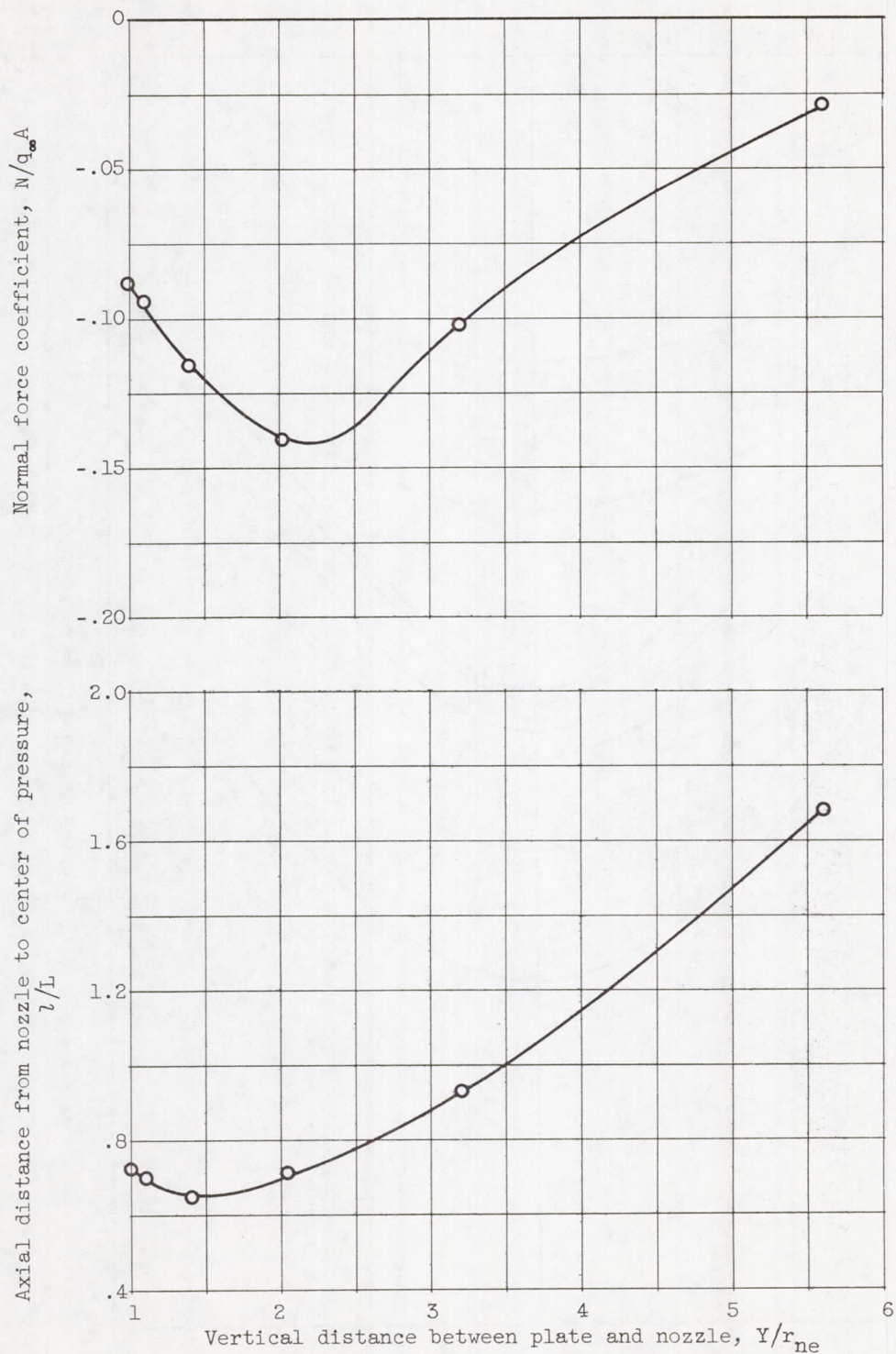


Figure 8. - Effect of vertical distance between plate and nozzle,  $Y/r_{ne}$ , on plate forces and moments. No fairing; jet velocity ratio,  $V_j/V_{\infty}$ , 0.85; pressure ratio,  $P/p_{\infty}$ , 2; free-stream Mach number, 1.6.

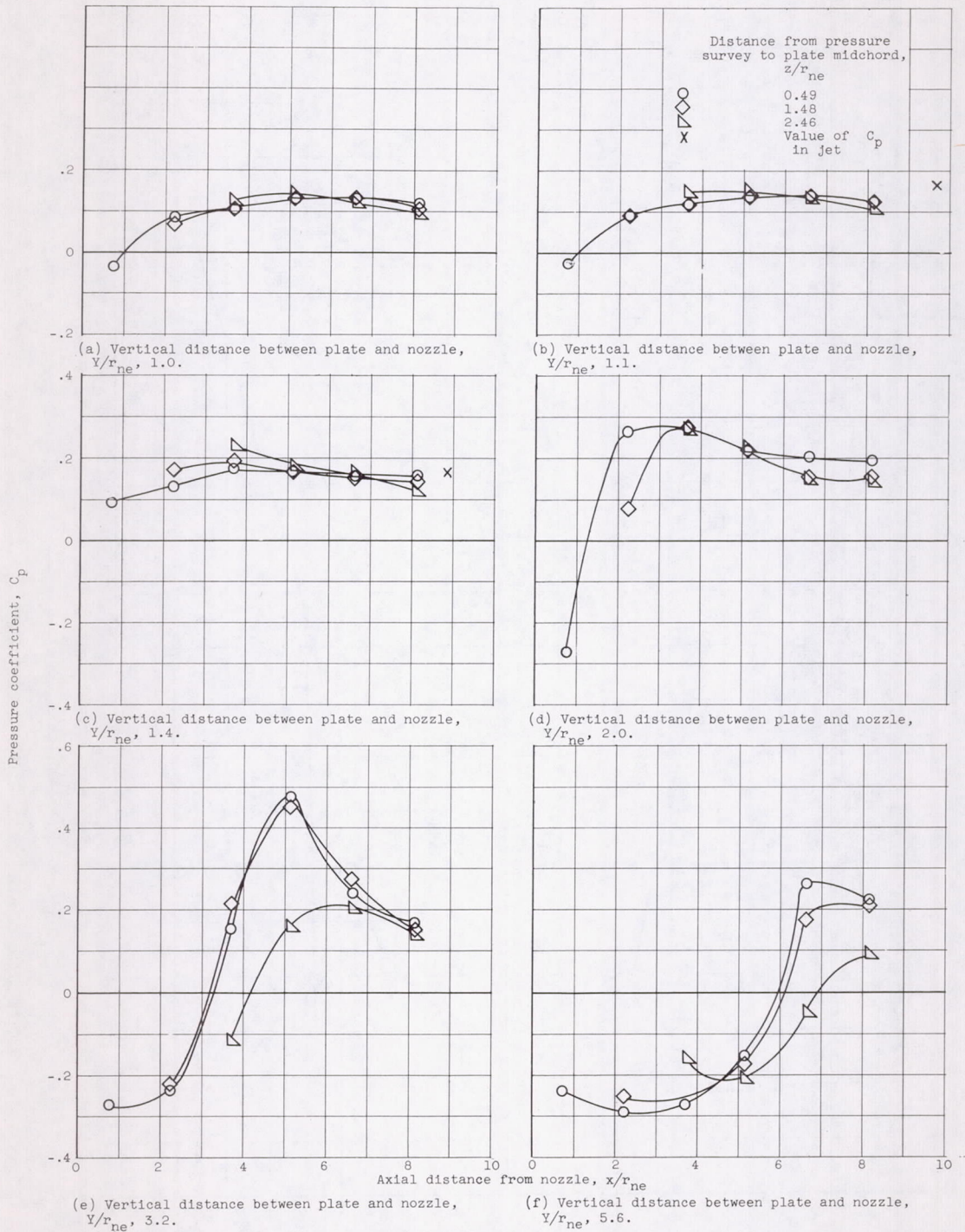
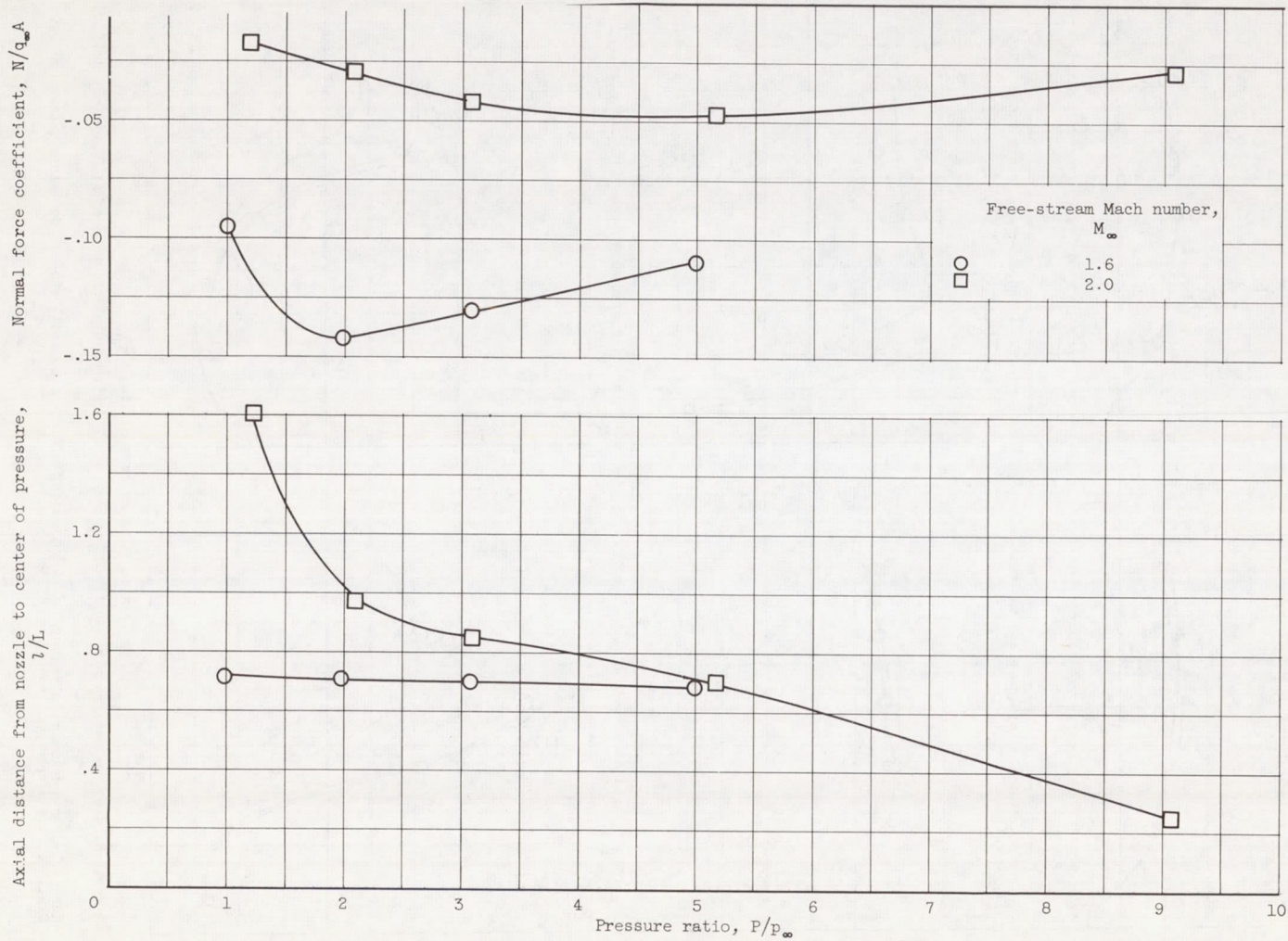
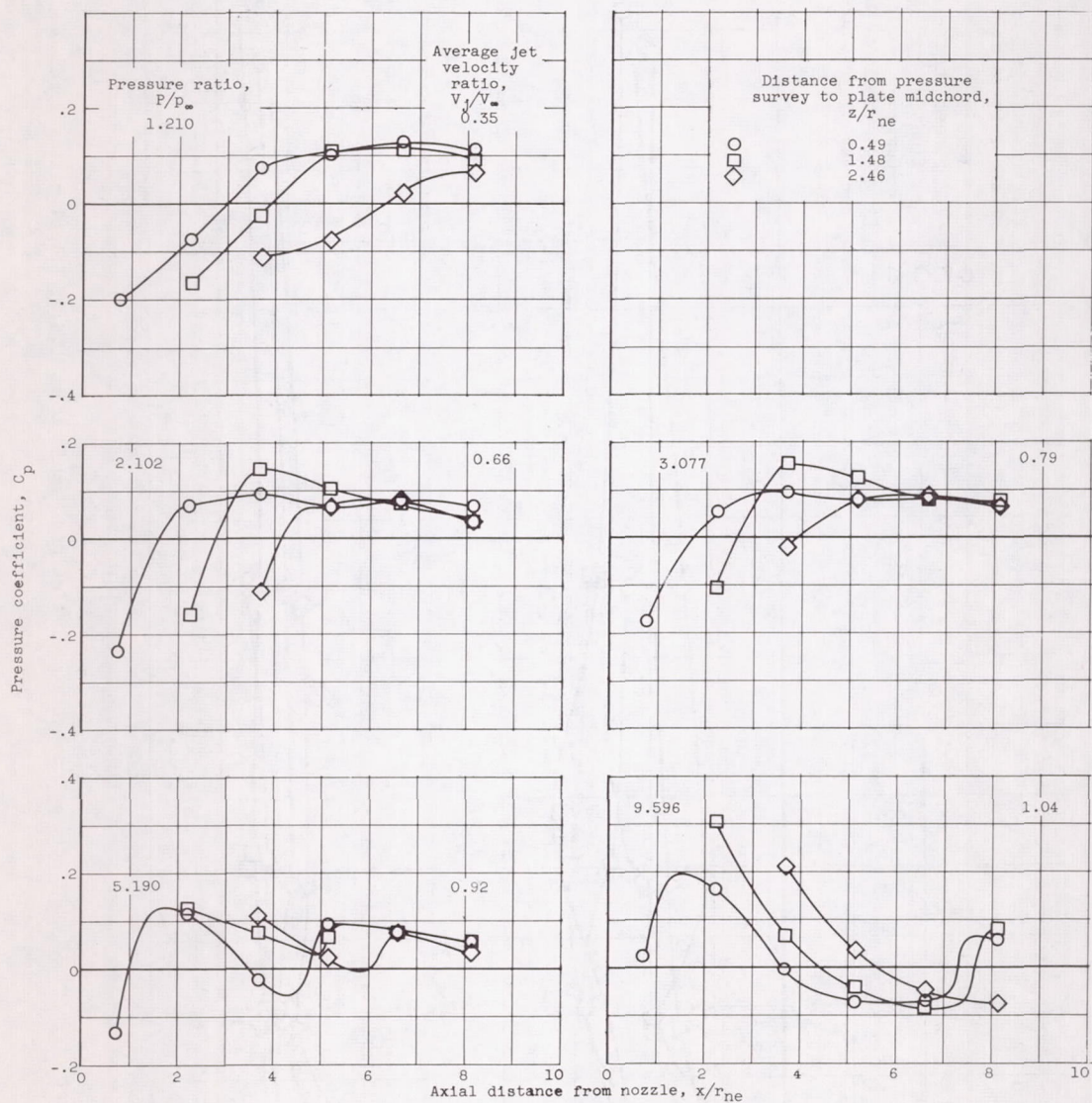


Figure 9. - Plate pressure distributions illustrating effect of boattail shock. No fairing; pressure ratio,  $P/p_\infty, 2$ ; free-stream Mach number, 1.6; jet velocity ratio,  $V_j/V_\infty, 0.85$ .



(a) Forces and moments.

Figure 10. - Effect of pressure ratio on plate pressure distribution, forces and moments. No fairing; vertical distance between plate and nozzle,  $Y/r_{ne}$ , 2.03.



(b) Pressure distribution. Free-stream Mach number, 2.0.

Figure 10. - Concluded. Effect of pressure ratio on plate pressure distribution, forces and moments. No fairing; vertical distance between plate and nozzle,  $Y/r_{ne}$ , 2.03.

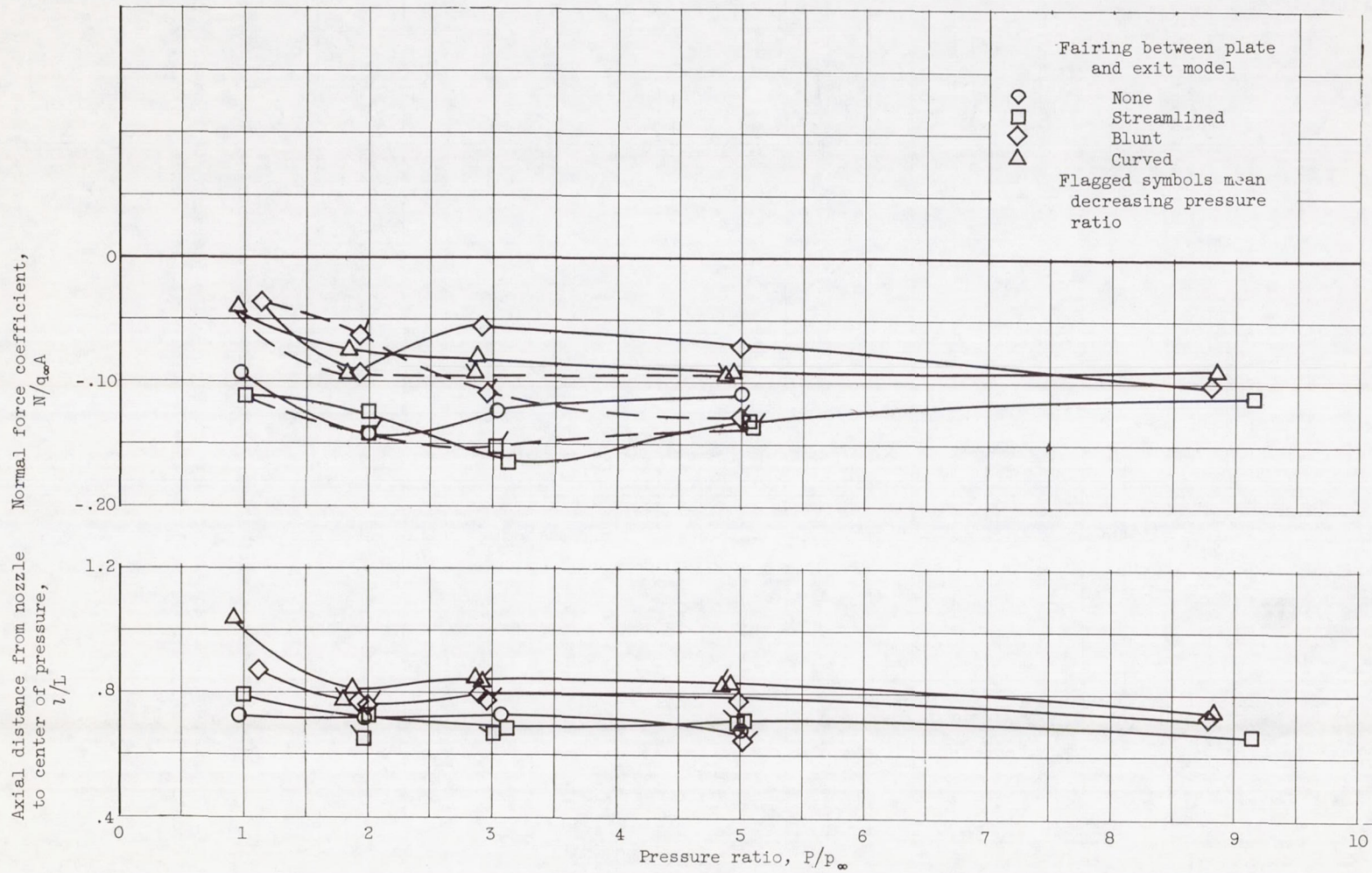


Figure 11. - Effect of fairings on forces and moments. Free-stream Mach number, 1.6; vertical distance between plate and nozzle,  $Y/r_{ne}$ , 2.03.

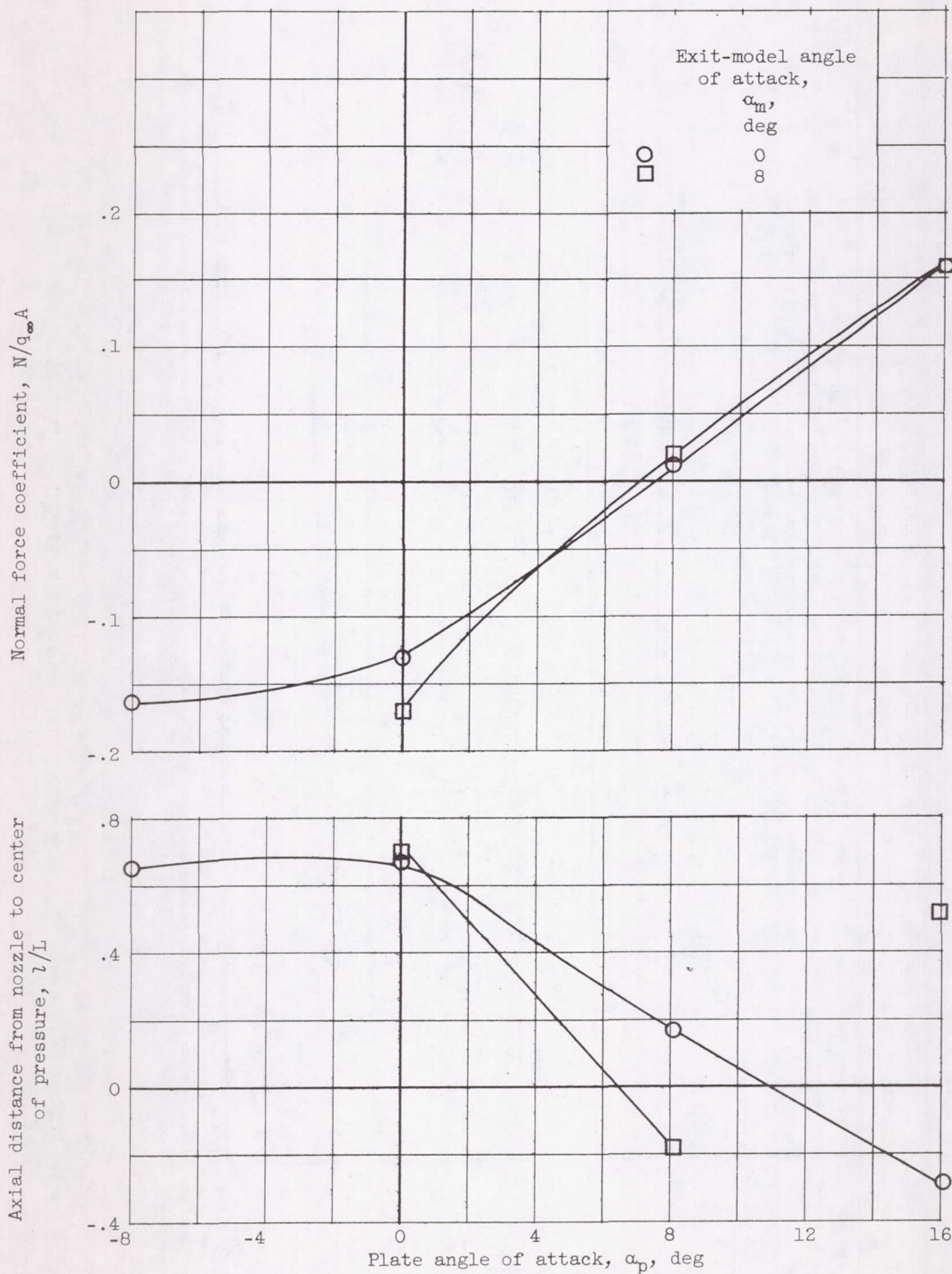
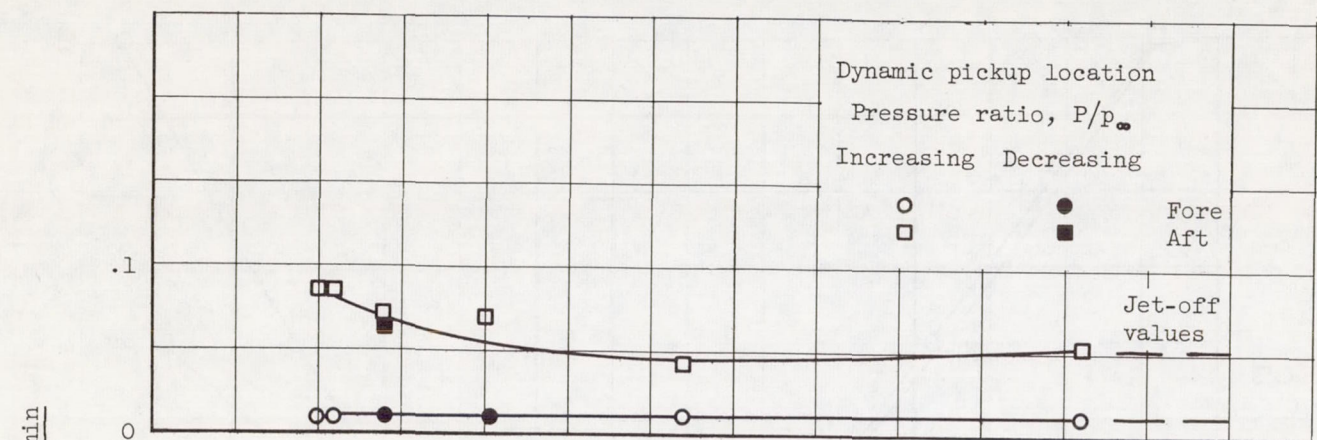
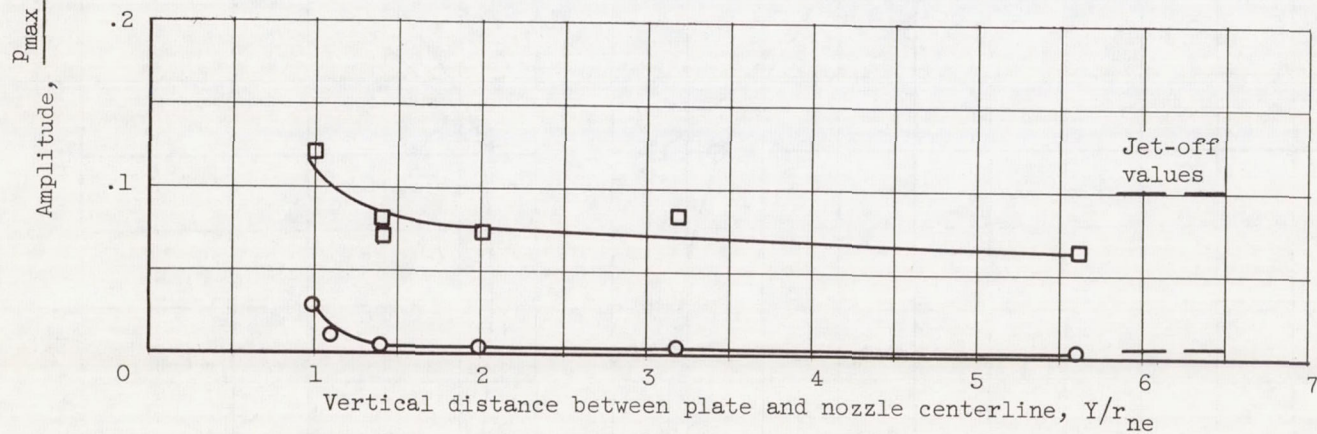


Figure 12. - Effect of plate angle of attack on forces and moments. Free-stream Mach number, 1.6; vertical distance between plate and nozzle,  $Y/r_{ne}$ , 1.4 at plate leading edge; pressure ratio,  $P/p_\infty$ , 2.0; jet velocity ratio,  $V_j/V_\infty$ , 0.85.





(a) Free-stream Mach number, 0.6; jet velocity ratio, 1.91.



(b) Free-stream Mach number, 1.6; jet velocity ratio, 0.85.

Figure 13. - Variation of pressure fluctuations with distance from jet. No fairing; pressure ratio,  $P/p_\infty$ , 2; average jet velocity ratio,  $V_j/V_\infty$ , 0.75.

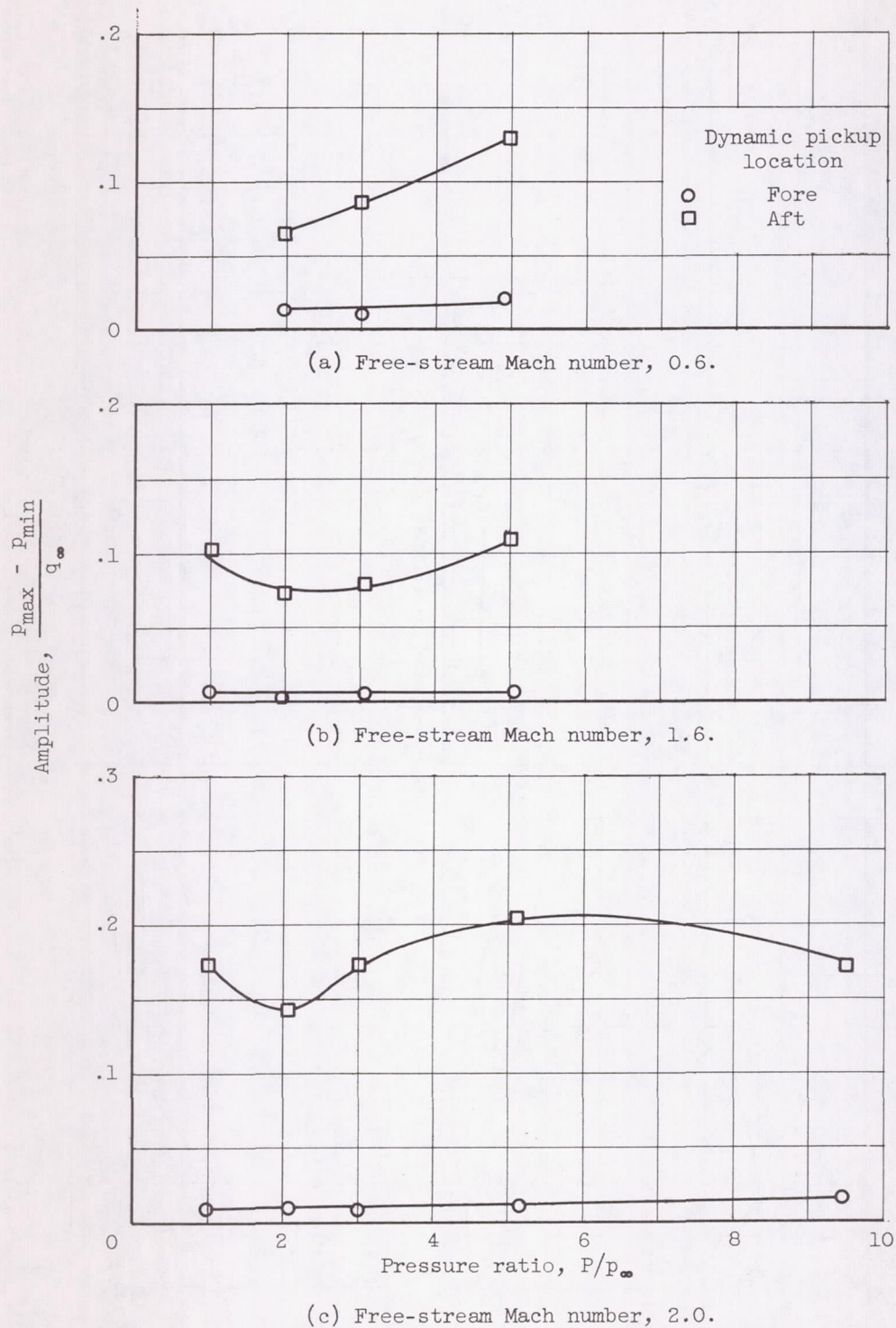


Figure 14. - Variation of pressure fluctuations with free-stream Mach number. No fairing; vertical distance between plate and nozzle,  $Y/r_{ne}$ , 1.4.

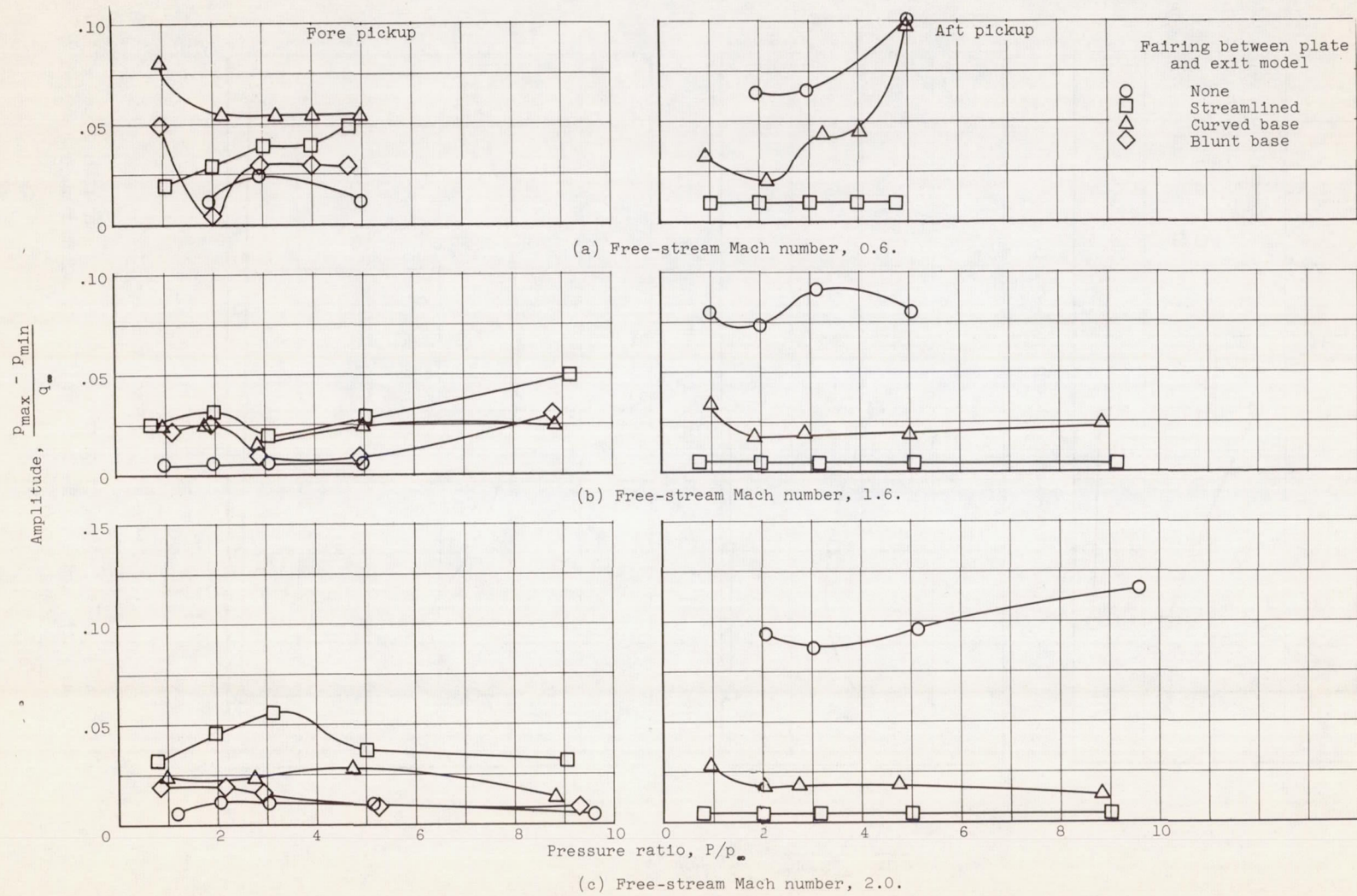


Figure 15. - Influence of fairings on plate pressure fluctuations.